

A SURVEY OF THE *EINSTEIN* IPC DATABASE FOR EXTENDED X-RAY SOURCESB. R. OPPENHEIMER¹ and D. J. HELFANDDepartment of Astronomy, Columbia University, 538 West 120th Street, New York, New York 10027
Electronic mail: bro@astro.caltech.edu, djh@carmen.phys.columbia.edu

E. J. GAIDOS

Center for Space Research, Massachusetts Institute of Technology, 77 Massachusetts Avenue, Cambridge, Massachusetts 02139
Electronic mail: ejgaidos@space.mit.edu

Received 1997 January 27; revised 1997 February 24

ABSTRACT

We present the results of a new analysis of the entire set of data collected by the Imaging Proportional Counter (IPC) on board the *Einstein* Observatory. Our survey is distinct from previous work such as the *Einstein* Extended Medium Sensitivity Survey (EMSS) in that it is designed to find extended sources and diffuse emission rather than point sources. In addition, the source detection algorithm is substantially improved over that used for the EMSS. We have searched for sources using circular apertures with variable radii up to $6.10'$. We have constructed criteria to ascertain which of the detections are truly diffuse and which of the sizes best approximates each detection. Using these criteria we have produced a catalog of 1326 extended source candidates at high Galactic latitude ($|b| > 20$ deg). Cross-correlating this list with existing source catalogs yields a reasonably comprehensive identification of the sources in our list. We find that over 400 are identified with known clusters of galaxies. Other objects are identified with galaxies, supernova remnants, AGN, and stars; the first two categories are often truly extended objects, while the latter two sets of objects can appear extended as a consequence of their soft X-ray spectra coupled with the broad point spread function of the IPC at low energies. A total of 321 extended sources remain unidentified. Many of these may be heretofore uncataloged clusters and groups of galaxies at moderate redshifts.

© 1997 American Astronomical Society. [S0004-6256(97)00606-7]

1. INTRODUCTION

Fifteen years ago, the *Einstein* Observatory completed a three-year program of pointed observations that provided the first arcminute-resolution images of the X-ray sky (Giacconi *et al.* 1979; Elvis 1990). All previous analyses of these data have employed search algorithms optimized for the detection of spatially unresolved sources. Of great importance in this regard are the Extended Medium Sensitivity Survey (EMSS) which provides a catalog of optically identified sources for a subset (one-third) of the IPC data (Gioia *et al.* 1990; Stocke *et al.* 1991), and the Two-Sigma Catalog of Moran *et al.* 1996 which extends this discrete source survey to a larger number of fields and to fainter flux levels. Clearly, however, the algorithm most sensitive to finding point-like sources will not be optimal for finding extended sources, and may miss a significant number of extended emitters altogether. For this reason we have designed a new source detection algorithm sensitive to emission from spatially resolved objects and have applied it to the complete set of 4100 IPC observations. Moran *et al.* 1996 provide a description of the point-source detection version of this algorithm and a detailed comparison of it with the EMSS algorithm. Here, we describe a survey of the IPC data which uses this algorithm

to find extended sources at high Galactic latitude. This new IPC catalog is then matched with other X-ray catalogs and catalogs at other wavelengths for confirmation and identification of its contents.

Besides the obvious motivation for this work—to complement the various existing point-source catalogs—our new catalog of diffuse and extended sources may be particularly useful in studies of X-ray galaxy groups and clusters. It also provides additional information about the completeness and systematics of the EMSS galaxy cluster catalog (Gioia & Luppino 1994) which has been the mainstay of studies of the X-ray evolution of these objects (e.g., Henry *et al.* 1992). The range of X-ray surface brightness which results from morphological variation and cluster evolution, as well as the finite angular resolution of the instrument, will introduce biases into any catalog and it is important to understand these effects. For example, clusters lacking peaked central emission as well as nearby, low-luminosity groups will both have more extended emission and be more likely to be recovered in this new catalog (Pesce *et al.* 1990). Furthermore, because our survey places fewer *a priori* constraints on the morphology and sizes of the sources it finds, the possibility of finding new types of diffuse X-ray sources exists. Tucker *et al.* 1995, for example, instituted a search for “failed clusters” by examining objects selected from the IPC catalog based on the relatively crude extent flag from the standard processing algorithm. They did detect eight previously uncatalogued

¹Current address: Department of Astronomy, California Institute of Technology, 105-24, Pasadena, CA 91125.

clusters, but owing to the relatively small number of objects studied (17) and the fact that nearly half of these were consistent with unresolved emission the significance of their results was limited.

In Sec. 2 of this paper, we describe the survey methodology, including the source detection algorithm, the procedures for removing duplicate and spurious sources, and the mechanism for selecting out extended sources. Section 3 briefly summarizes the statistics of the identified component of the catalog, while Sec. 4 discusses comparisons with the Einstein Extended Medium Sensitivity Survey (Gioia *et al.* 1990) and the *ROSAT* All-Sky Survey (Voges *et al.* 1996), and offers a few comments on the utility of our new catalog. We conclude with a summary of this work and access information for those interested in using the catalog.

2. THE SURVEY METHODOLOGY

2.1 Source Detection Algorithm

A survey of this nature requires the construction of a detection algorithm sensitive to faint, diffuse sources. The algorithm we use is a slightly modified form of the one implemented by Moran *et al.* (1996) to generate the *Einstein* Two-Sigma Catalog. Briefly, the distinctions between our procedures and the standard *Einstein* processing system include the application of a flat field to compensate for IPC detector nonuniformities, improved data editing, a circular (rather than square) source aperture, a local background determination for each search cell, and an iterative source search algorithm using apertures of different size.

We surveyed the IPC data four times, each time for a different source size, or detection aperture. For each aperture, we kept a record of every source detected with a significance of greater than 2.5σ . The source acceptance threshold for each aperture is actually higher than this, but this information is retained for subsequent tests of source extent.

The smallest aperture we used has a radius of $1.25'$, the optimal size for a point-source, as determined by the point spread function of the IPC (see Hamilton *et al.* 1991 for a justification of this choice); the background annulus extends from $3'$ to $6'$ as in Moran *et al.* (1996). The other three apertures have radii of $2.35'$, $4.20'$, and $6.10'$. The four aperture radii represent a rough linear progression in their square roots, with some rounding due to the image pixel size. The background annuli for these large apertures are correspondingly larger such that the area in the annulus (and, thus, the statistical uncertainty in the background determination) is roughly the same for all four apertures. For the $1.25'$ aperture search we employed images with $32''$ pixels; the data were rebinned into $64''$ pixels for the three larger aperture iterations.

An extended source detected in the four apertures ought to show an increase in significance out to the limiting radius of the object, beyond which, the significance should drop rapidly as more background flux is included in the source aperture. Thus, by examining the progression of the signal-to-noise ratios for a given source as it is detected in each of the four apertures, we can ascertain whether the source's X-ray emission is point-like or extended.

An alternative technique to this multiple aperture photometry is to use a pre-determined two-dimensional source profile (e.g., an elliptical Gaussian) to find and fit locations of significant X-ray emission. However, we feel that our approach is less likely to introduce biases into the detection process by assuming a particular form of source profile and is more appropriate to an application with high photon noise and large computational overhead.

2.2 Removal of Spurious and Duplicate Sources

After generating four large lists of source candidates greater than 2.5σ above background (one for each aperture), we proceeded to limit the number of spurious sources and, for a source that appears in more than one of the four lists, to decide which sky position to use to represent the source in the final catalog. We did this in several steps.

First, we have adopted the same requirements as Moran *et al.* (1996) for the minimum number of usable pixels (i.e., those outside the IPC window support ribs and uncompromised by the presence of a nearby source) in both the source aperture and the background annulus required to admit a candidate to the final source list: 60% and 30% of the full areas, respectively. As described in that paper, these requirements result in a significant reduction in spurious detections. To reduce further the number of spurious detections, we only used data within the central $38' \times 38'$ of the detector bounded by the window support ribs. In the outer regions of the IPC, the ratio of X-rays to non-X-ray background falls significantly, and large numbers of spurious, low-significance sources swamp the few real detections.

A third and obvious method for the removal of spurious sources is to increase the signal-to-noise ratio threshold. To this end, a plot of detected source positions as a function of IPC instrumental coordinates is useful. For real celestial sources, such a plot should exhibit an excess of detections at the field center, along with a quasi-random distribution of sources scattered over the rest of the field. The central enhancement is a result of the fact that most pointings were targeted at known or suspected X-ray sources. The quasi-random component of the distribution, due to serendipitously detected sources, should show an enhanced source density in regions where the instrument is more sensitive, i.e., where the flat-field correction is larger.

Figure 1 shows such plots for all detections in each of the four catalogs. Apertures 1 and 2 (with $1.25'$ and $2.35'$ radii) exhibit some of the more prominent features of the flat-field such as the enhanced sensitivity along the vertical band near the left edge and just to the right of the center (see Fig. 4 in Moran *et al.* 1996 for a greyscale plot of the flat-field.) These features are, as expected, more difficult to see in the plots of detections for the two larger apertures, because the aperture size tends to wash out the arcminute-scale detail. Of note in these plots is a distinct clumping of detections in the corners of the detector. These are primarily spurious detections, an artifact of the local background subtraction technique which begins to fail at field edges where the numbers of usable pixels in both the source aperture and the background annulus are near the limits set by the algorithm. Figure 2 demonstrates the effect of increasing the minimum significance re-

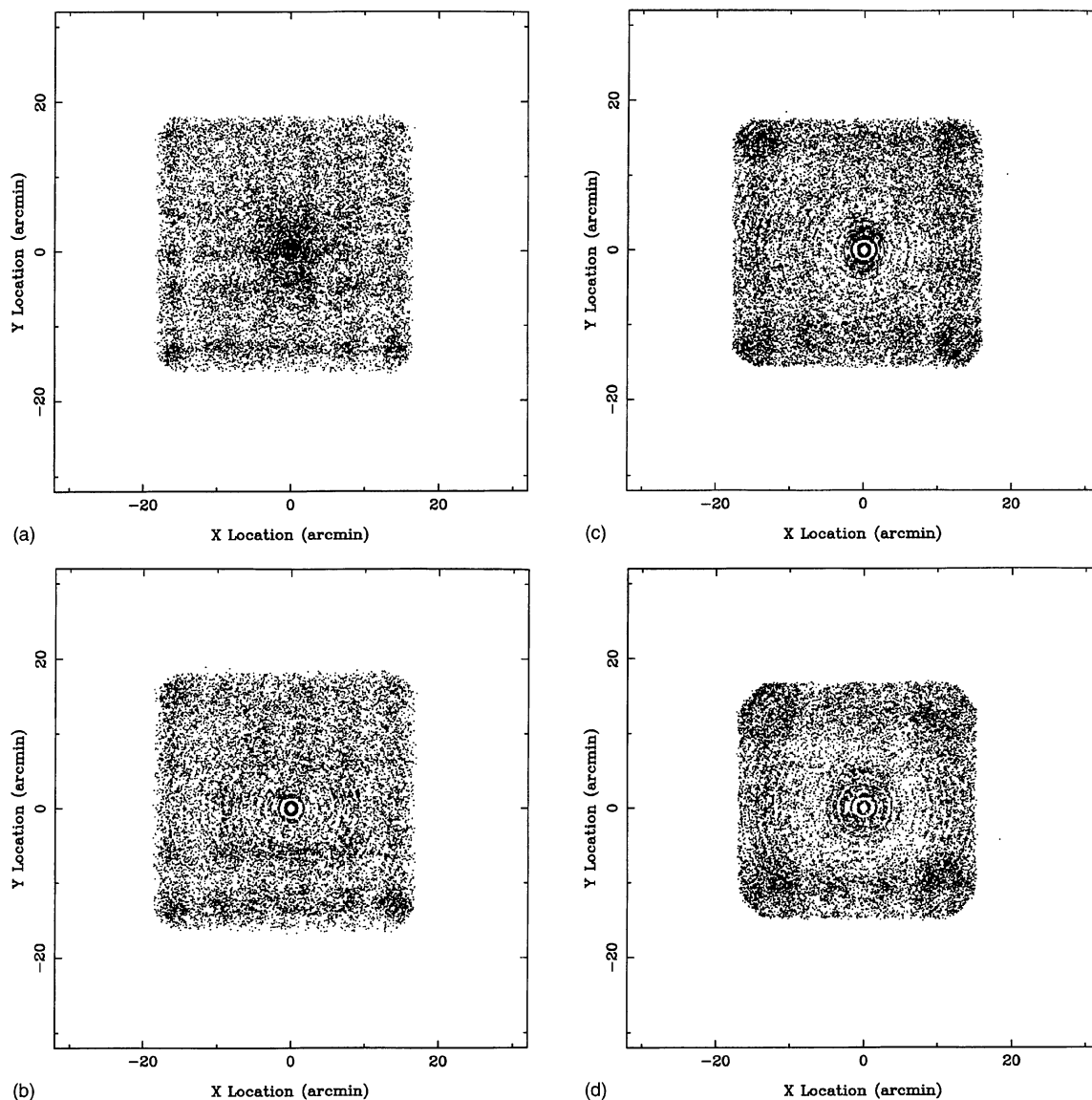


FIG. 1. Locations of source detections greater than 2.5σ on the face of the IPC instrument. (a) 15456 detections with aperture 1, (b) 15265 detections with aperture 2, (c) 16567 detections with aperture 3 and (d) 14048 detections with aperture 4. The circular patterns are a consequence of pixel quantization of positions.

quirement on these detections. The first plot shows the aperture 3 ($4.20'$ radius) detections greater than 4.5σ above background. The second plot shows aperture 4 ($6.10'$ radius) detections above 5σ . The excess detection density in the field corners has essentially vanished in these plots, indicating that many spurious detections have been removed.

By examining many plots such as those in Fig. 2 with varying signal-to-noise ratio thresholds, we decided to retain any detection such that the aperture 1 ($1.25'$) signal is greater than 3σ , the aperture 2 ($2.35'$) signal is greater than 4σ , the aperture 3 ($4.20'$) signal is greater than 4.5σ , or the aperture 4 signal ($6.10'$) is greater than 5σ . The final catalog of sources, however, includes only those which have detections in at least two of the three larger apertures. This intermediate

step, in which we also include the sources that appear in aperture 1, allows us to characterize the differences between point-like and extended sources (see Sec. 2.3).

We next removed overlapping detections and combined the four separate catalogs into one master database of sources. Within each of the four catalogs individually, we ascertained which detections overlapped each other based on the aperture radius. We retained only the one source with the highest signal-to-noise ratio in each set of overlapping sources. We then constructed a catalog by combining spatially coincident detections from the four individual aperture catalogs. For each source, a position is listed, along with the signal-to-noise ratio and the flux calculated in each of the four apertures (with a null value listed when a given source was not detected in a particular aperture). Again, in cases

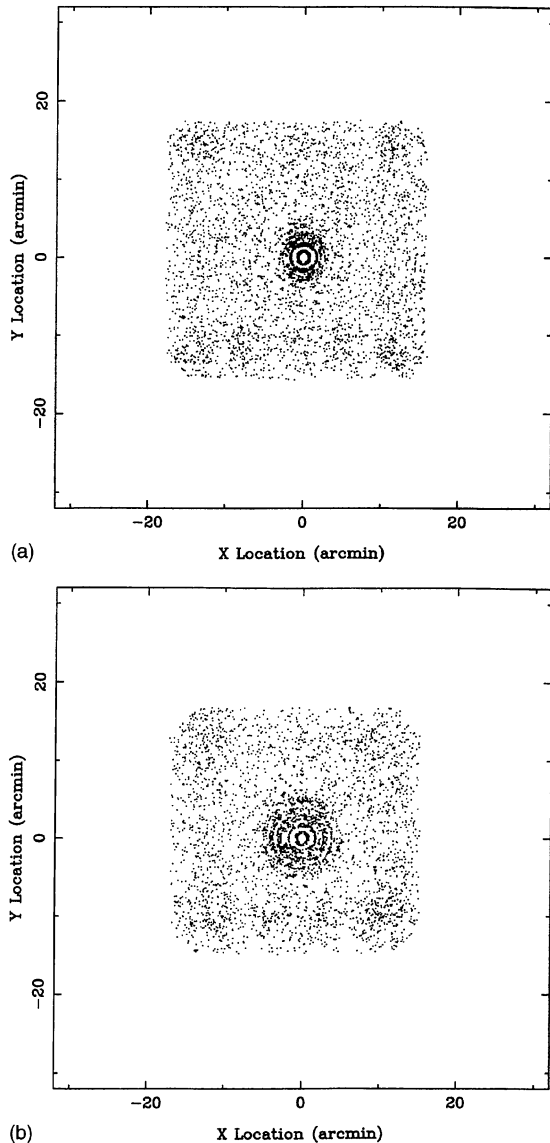


FIG. 2. Locations of source detections on the face of the instrument. (a) 4505 sources greater than 4.5σ detected with aperture 3 and (b) 3740 sources greater than 5σ detected with aperture 4.

where multiple small aperture detections coincided with a large aperture detection, only the highest signal-to-noise detection of the multiple smaller aperture detections was retained. The sky position of each source is the weighted average of the positions of all the detections. The weighting factor is r_i^2/σ_i^2 , where r_i is the radius of aperture i , and σ_i is the signal-to-noise ratio measured for aperture i .

The source catalog was then culled by excluding IPC fields within 20 degrees of the Galactic plane or whose average photon-counting rates exceeded $3 \text{ counts sec}^{-1}$. There are three reasons for the high-flux exclusion. First, such fields may include bright, well-studied diffuse X-ray sources. Second, they may contain very bright point sources with significant non-Gaussian point-spread-function wings arising from scattering of the incident X-rays off mirror imperfec-

tions. These sources are not effectively removed by the source excision algorithm in the search program, and result in spurious detections of diffuse sources. Third, these high-flux fields may have high non-X-ray background rates which also enhance the false source detection rate. Additionally, many nearby (i.e., large) extragalactic objects have diffuse X-ray emission and produce spurious detections that could be identified as extended sources. Therefore, any sources within 5° of the Large Magellanic Cloud, 2.67° of the Small Magellanic Cloud, 2.67° of the Coma Cluster, or 1.6° of Messier 31 were excluded. The final product is a 7419-entry master catalog. (The full version of this catalog is available in electronic form at <http://astro.caltech.edu/~bro.>)

2.3 Selecting Extended Sources

In order to produce a scheme by which we might distinguish a truly diffuse source from a point source, we take advantage of the great effort expended over the last fifteen years in identifying IPC X-ray sources (e.g., Stocke *et al.* 1991 and references therein). Specifically, we matched our list of 7419 sources with the 2E Catalog available from the Harvard-Smithsonian Center for Astrophysics via EINLINE. All matches were recorded, along with the difference in position between our detection and the EINLINE catalog entry. A total of 241 stars and 193 quasars were identified within $1.5'$ of our positions. This radius is roughly consistent with the point-source size determined by Hamilton *et al.* (1991), and an examination of the distribution of offsets of EINLINE sources from our sources shows a strong peak with a width of about $1.5'$ radius. Furthermore, 484 sources in our master catalog were identified with galaxy clusters within $6.2'$ (370 within $4.1'$; although there are only 268 galaxy clusters identified as such in EINLINE, several of them were detected multiple times because of their large sizes). Virtually all of the identifications in the 2E catalog are a result either of the detection of the pointing target or of individual spectroscopic followup of serendipitous sources (rather than simply matching catalogs of objects from other wavelength regimes). Therefore, the false identification rate is very low. As a consequence, by comparing how the σ_i values for a known point source (i.e., a star or quasar) behave as i increases with the behavior of the σ_i values for known extended sources (i.e., galaxy clusters), we can develop criteria for distinguishing unidentified point sources from unidentified extended sources. To this end, we define the quantity $\sigma_{ij} = \sigma_i/\sigma_j$, the ratio of a source's σ values in two different apertures. These six ratios provide a simple means for determining the behavior of signal-to-noise ratio as a function of aperture size.

In Fig. 3, we compare the normalized σ_{ij} distributions for stars and quasars. The two are strikingly similar, as expected for two sets of objects that are both unresolved in the IPC. There are small, statistically insignificant differences in the mean values for several of the distributions (see Table 1). These differences are, however, in the sense expected in that they reflect the spectral difference between the two source classes: stars, with softer spectra on average, produce broader point-spread-function distributions due to the poorer electron cloud localization in the IPC for low-energy pho-

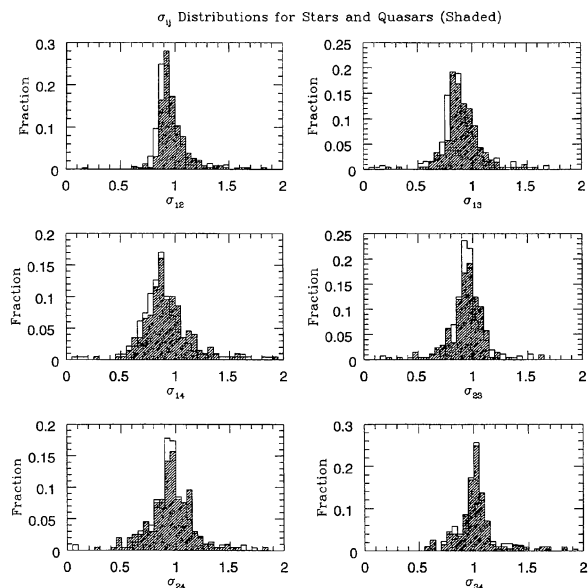


FIG. 3. Normalized distributions of σ_{ij} for sources identified as stars and quasars by EINLINE. The shaded histogram indicates the distribution for quasars. The unshaded histogram corresponds to the stars.

tons. Given the small differences these spectral distinctions make, as well as the fact that the extended sources for which we are searching can be expected to have a wide variety of spectral temperatures, we sum the σ_{ij} distributions of these two source types to produce our point-source template distributions.

Figure 4 displays these point-source distributions plotted together with our measurements of the σ_{ij} distributions for the galaxy clusters found in the 2E catalog. The dramatic difference is immediately apparent. The cluster distributions are much broader, reflecting the range of intrinsic cluster X-ray emission profiles, and the means are at much lower values (Table 1), demonstrating the increase in signal-to-noise as more source flux is included as the aperture size increases (and less source flux is included in the background annulus).

In order to isolate extended sources in the catalog, we derive criteria for separating point-like and extended sources using these σ_{ij} distributions. The intention is to produce a final catalog of extended source candidates with minimal contamination by point sources. We choose to be conservative, sacrificing possible extended sources for the sake of a more finely distilled catalog free of point sources. We assign ‘‘cutoff ratios’’ for the σ_{13} , σ_{14} , and σ_{24} distributions for which the point-source distributions are quite well separated from the cluster distributions. The ‘‘cutoff ratios’’ were selected by choosing the point in the plots in Fig. 4 where the

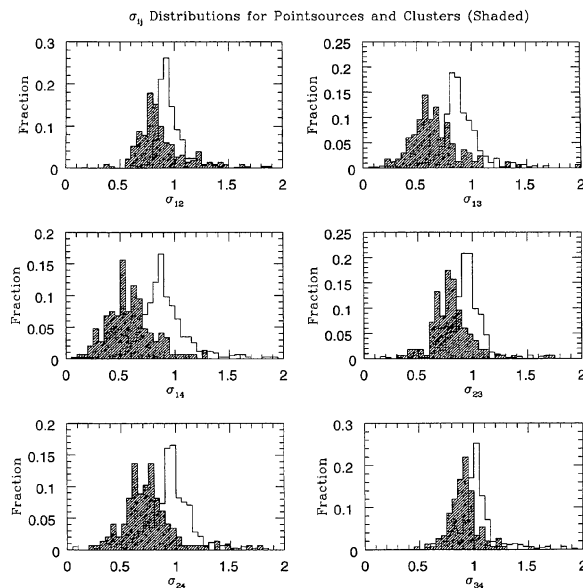


FIG. 4. Distributions of σ_{ij} for sources identified in EINLINE as galaxy clusters (shaded histogram) and as point-sources (the sum of the two histograms in Fig. 3).

point source distribution crosses the cluster distribution. This effectively treats the distributions as probability distributions. Thus, in the region below the ‘‘cutoff ratio’’ a given source is more likely to be extended than point-like. The ‘‘cutoff ratios’’ used are 0.75, 0.70, and 0.85, respectively. In Sec. 4 we estimate the degree of contamination by point sources in the final catalog.

The result of applying these cutoff ratios to our master catalog is the *Einstein* eXtended Source Survey (which we dub the EXSS). To produce the EXSS, we took a source from the master catalog only if it obeyed the following set of rules: (1) it appears in all four apertures and has σ_{13} , σ_{14} , and σ_{24} which are less than the corresponding ‘‘cutoff ratios’’; or (2) it appears in at least two of the three largest apertures and still obeys the applicable ‘‘cutoff ratios.’’ No sources detected only in aperture 1 were retained. The EXSS catalog contains 1326 sources: The 333 sources appearing in only one of apertures 2, 3, or 4 were set aside in a separate list. These catalogs can be obtained in electronic form at <http://astro.caltech.edu/~bro>.

3. IDENTIFICATION OF EXTENDED SOURCES

Obtaining the Abell and Zwicky catalogs of galaxy clusters from the High Energy Astrophysics Science Archive Research Center (HEASARC), we identified every EXSS source within $12'$ of the central position of an Abell cluster

TABLE 1. Mean values of σ_{ij} distributions.

Object Type	$\langle\sigma_{12}\rangle$	$\langle\sigma_{13}\rangle$	$\langle\sigma_{14}\rangle$	$\langle\sigma_{23}\rangle$	$\langle\sigma_{24}\rangle$	$\langle\sigma_{34}\rangle$
Stars	0.95 ± 0.06	0.89 ± 0.05	0.92 ± 0.06	0.96 ± 0.06	1.00 ± 0.07	1.08 ± 0.07
Quasars	1.00 ± 0.07	0.92 ± 0.06	0.93 ± 0.07	0.94 ± 0.07	0.96 ± 0.07	1.03 ± 0.07
Clusters	0.88 ± 0.06	0.70 ± 0.08	0.62 ± 0.08	0.82 ± 0.08	0.76 ± 0.08	0.93 ± 0.08

or closer to a Zwicky cluster than the quadrature sum of $6'$ and the size of the cluster listed in the Zwicky catalog. A total of 273 sources were coincident with Abell Clusters and 120 with Zwicky Clusters. Forty-seven sources were identified through cross-correlation with the EMSS catalog and 183 with the EINLINE catalog. Cross-correlation with the Positions and Proper Motions catalog (Röser & Bastian 1991) found 115 sources coincident to within $3.0'$ of stars.

In an attempt to identify the remaining 835 unidentified, extended X-ray sources, we queried the NASA/IPAC Extragalactic Database (NED). We searched with a $12'$ radius at each position in our catalog. The result was that, of the 835 sources, some 150 contained galaxies that belong to known galaxy clusters, groups or sets of interacting galaxies, including Southern Clusters, clusters in the Catalog of Galaxies and Clusters of Galaxies, Arp's Peculiar Galaxies and the outlying galaxies of some Abell and Zwicky clusters that were not within the radii used above to match Zwicky and Abell Clusters with EXSS sources. Another 323 sources contain one or more galaxies (as found by NED), 37 contain quasars, and 4 are associated with H II regions. As a result of this elaborate exercise in cross-correlation, the catalog retains 321 unidentified sources. These we put forth as the unidentified subset of the EXSS (see Table 2).

Of these 321 unidentified X-ray sources, 124 contain known radio sources and 47 contain known infrared sources (with some overlap between the two sets); 163 contain no cataloged objects in any other wavelength band. We consider the sources which contain infrared sources and radio sources to be unidentified in the sense that their astrophysical nature is unknown. Furthermore, most of these cases can be explained by chance coincidence. The 321 sources searched for in NED cover about 40 square degrees on the sky. With 2.86 Greenbank sources per square degree (Gregory & Condon 1990) and 2 *IRAS* sources per square degree outside the Galactic plane (Beichman *et al.* 1988), we would expect to find about 80 ± 9 *IRAS* sources and about 115 ± 11 Greenbank sources within the bounds of our X-ray sources. Thus the frequency of matches between the X-ray and radio catalogs can be entirely explained by random coincidences.

Table 2 presents a full listing of the 321 unidentified EXSS sources. The table lists for each source the weighted-average position (as described above), the largest signal-to-noise ratio at which it was detected, the radius of the aperture with which that detection was made, and the flux in counts per second measured through this aperture. The radius can be considered a very crude estimate of the source angular extent. In addition, the last field in the table indicates what, if any, type of source (radio or infrared) exists within the unidentified EXSS source region.

4. COMPARISON WITH OTHER X-RAY SOURCE CATALOGS

A comparison between the EXSS catalog generated here and the EMSS catalog can be used to assess the importance of our reduced systematic errors and a detection routine less susceptible to surface-brightness selection in the re-analysis

of the IPC data. The proper evaluation of these effects is an integral part of the interpretation of catalogs such as the EMSS which are taken to be complete.

First we cross-correlated the master catalog with the EMSS. Some 607 of the 835 EMSS sources are identified with sources in our master catalog. (The other 228 sources were not found because they lie outside the rib structure of the IPC, areas excluded from our search but partially included in the construction of the EMSS catalog.) In Fig. 5 we have plotted our best signal-to-noise ratio versus the EMSS signal-to-noise ratio for each of these 607 sources. Symbols denote which aperture yielded the best signal-to-noise ratio in our search. Virtually every point in the plot lies above the line of equality. At the low σ end, a few points fall below the line, but these are low-significance sources whose signal-to-noise ratios are very sensitive to the detection algorithm used. Above 10σ on the σ_{EMSS} axis, only three points fall below the line of equality. The two near $\sigma_{\text{EMSS}}=18$ (MS 0134.4+2027 and MS 1332.6-2935) are sources that are half-observed by the rib at the edge of the field we searched. These objects have slightly reduced signals because they are partially cut out by the EXSS search scheme which does not use data under the ribs. The aperture 4 size source below the line at $\sigma_{\text{EMSS}}=13$ corresponds to the EMSS source MS 1701.5+6102. This object appears in several different IPC observations. The exposure with the longest integration time has the object outside the rib structure, and is the one which the EMSS used to make its measurements. Since we were restricted to sources within the ribs, we had to use an exposure with a shorter integration time, leading to an entry with a lower signal-to-noise ratio in our catalog. The same circumstances might explain some of the other, lower-significance points that lie below the line along which σ equals σ_{EMSS} .

Figure 5 demonstrates clearly that our improved analysis of the data has yielded substantial gains in sensitivity. Furthermore, the use of multiple apertures is shown to be beneficial: Most of the aperture 1 sources are near the line of equality, while the larger aperture sources are detected at greater significance. For example, we find an average increase of 45% in signal-to-noise ratio for 79 galaxy clusters first detected in the EMSS. Some of these clusters were detected at significance levels 2.5 times higher than their EMSS detections. These successes bode well for our search for X-ray selected clusters amongst the unidentified component of the EXSS.

Figure 6 shows a plot similar to that of Fig. 5, but in this case, only sources that pass the requirements for being extended are included. In this plot only two points lie below the line. These are both a result of partial obscuration by the ribs. In this plot, circles surround the points that correspond to galaxy clusters. These are consistently detected with much greater signal-to-noise ratios in our survey.

This comparison with the EMSS permits an estimation of the contamination by point sources in the EXSS. In the mas-

TABLE 2. Unidentified sources in the *Einstein* Extended Source Survey.

R.A. (1950): ^h	^m	^s	Dec. (1950): ^o	[']	["]	Ap.	Flux	σ	ID
0	4	34.34	15	49	8.0	4	0.026	4.72	Radio
0	14	10.95	16	13	38.2	3	0.010	5.02	IR
0	18	50.31	1	16	5.8	4	0.031	5.29	Radio
0	19	50.10	-12	45	5.0	4	0.023	5.34	Radio
0	20	0.16	-12	19	34.1	3	0.017	4.56	none
0	26	40.14	88	36	48.9	4	0.024	5.71	none
0	26	45.45	6	9	23.4	4	0.054	5.16	none
0	32	42.85	-7	43	39.3	4	0.049	5.15	IR
0	35	29.21	29	33	48.3	4	0.039	6.73	none
0	37	59.62	40	12	53.7	4	0.016	5.70	Radio
0	39	3.75	40	28	40.2	3	0.008	5.49	Radio
0	42	38.18	0	50	13.6	3	0.050	5.07	Radio
0	45	1.61	24	14	20.3	3	0.032	4.95	Radio
0	45	47.53	-12	13	53.9	3	0.034	4.56	IR
0	49	6.46	88	50	48.7	4	0.020	5.32	IR
0	56	39.04	29	59	18.5	3	0.011	4.86	none
1	4	37.66	-21	39	41.0	4	0.026	4.68	none
1	7	8.16	14	55	13.2	4	0.053	5.29	none ^a
1	14	55.00	-1	3	4.2	4	0.020	5.42	none
1	16	40.61	0	-57	2.3	4	0.028	5.91	none
1	17	17.99	8	14	54.7	4	0.014	6.15	Radio
1	20	32.45	-3	36	21.1	4	0.026	5.80	Radio
1	21	44.20	7	0	4.4	3	0.029	4.31	Radio
1	22	10.80	23	22	2.6	4	0.055	5.50	Radio
1	22	47.94	19	5	47.7	3	0.026	5.98	Radio
1	33	5.48	15	27	15.3	3	0.016	4.65	none
1	34	48.17	-5	4	35.9	4	0.063	6.53	IR
1	34	51.85	15	21	31.4	4	0.022	5.09	none
1	35	1.84	20	32	24.9	3	0.014	4.53	none
1	37	24.49	-18	22	12.3	3	0.023	4.90	Radio
1	38	50.29	4	27	34.9	4	0.044	6.38	Radio
1	39	14.88	-30	25	7.4	3	0.018	6.10	none
1	58	9.75	12	48	26.7	3	0.020	4.50	none
1	59	22.57	-8	51	32.7	3	0.017	4.52	none
2	3	48.39	23	16	32.0	4	0.021	6.25	none
2	4	26.69	-37	50	10.8	4	0.038	5.72	Radio
2	15	1.48	-51	32	13.6	4	0.055	5.63	none
2	24	55.31	-10	41	38.3	4	0.029	6.83	none
2	27	40.80	-12	54	26.1	4	0.052	5.11	none
2	36	46.03	16	33	10.3	4	0.047	5.11	none
2	40	6.10	6	47	10.2	3	0.027	5.68	none
2	55	43.32	20	41	55.6	4	0.033	5.51	none
2	58	3.03	7	29	28.7	3	0.019	5.22	none
2	59	42.27	-14	48	3.3	4	0.026	5.46	IR
3	4	12.56	15	23	7.7	3	0.014	4.82	none
3	5	19.02	-12	26	16.1	3	0.027	4.76	none
3	5	32.87	10	26	10.5	4	0.050	5.49	Radio
3	9	19.88	14	41	46.4	3	0.011	4.81	none
3	24	37.76	28	23	37.3	3	0.029	4.82	Radio
3	30	26.22	-9	20	38.8	3	0.059	4.71	none
3	32	6.44	-26	2	9.7	4	0.073	5.24	Radio
3	44	13.75	-25	8	23.1	4	0.060	5.39	IR
3	46	33.64	23	17	28.7	3	0.033	6.73	none
3	46	35.40	17	17	28.4	4	0.061	6.34	Radio
3	52	20.65	2	50	26.4	4	0.071	5.80	none
3	58	46.53	10	25	36.2	3	0.028	4.55	none
4	1	20.22	-36	32	8.8	3	0.034	4.80	none
4	6	26.04	-12	20	50.5	3	0.046	4.71	none
4	10	6.17	7	37	54.6	4	0.038	5.97	none
4	15	26.29	-6	11	53.7	4	0.031	5.15	none
4	15	30.03	-5	49	13.1	3	0.029	4.58	none
4	21	23.31	0	27	31.7	4	0.051	5.36	Radio
4	31	12.13	5	30	30.4	3	0.010	5.05	IR
4	31	33.13	5	8	15.0	3	0.010	5.75	none
4	33	14.13	10	19	39.0	4	0.047	5.17	none
4	33	18.14	-10	21	2.5	4	0.079	5.11	none
4	38	41.93	-15	39	36.0	4	0.023	5.25	none

TABLE 2. (continued)

R.A. (1950):	<i>h</i>	<i>m</i>	<i>s</i>	Dec. (1950):	$^{\circ}$	<i>'</i>	<i>"</i>	Ap.	Flux	σ	ID
4	39	22.40		-16	10	17.3		3	0.009	5.64	Radio
4	40	47.34		8	28	50.3		4	0.034	5.30	none
4	45	1.94		-59	37	9.0		4	0.033	6.25	none
4	46	52.27		-59	9	8.3		3	0.025	4.98	Radio
5	2	10.88		-11	54	2.6		4	0.020	6.18	none
5	2	13.55		-12	1	18.3		3	0.017	6.02	none
5	3	35.44		-11	44	9.4		4	0.021	5.58	none
5	9	34.71		-44	57	38.5		3	0.036	4.57	none
5	13	2.88		-8	13	22.3		4	0.043	5.49	IR
5	38	51.76		-44	0	47.3		4	0.033	4.70	none
6	1	9.05		-31	58	52.4		4	0.063	5.50	none
6	14	10.12		-59	8	15.1		4	0.028	5.56	IR
6	14	39.71		-59	23	41.5		4	0.028	5.54	IR
6	15	42.30		-59	32	14.8		3	0.019	4.52	Radio
6	26	35.32		-55	11	11.4		4	0.021	5.26	none
6	35	54.74		-75	32	41.0		4	0.055	4.64	none
6	43	41.43		53	17	36.4		4	0.043	5.07	IR
7	33	44.40		65	30	56.5		3	0.018	4.91	Radio
7	39	42.54		37	46	51.3		3	0.011	4.83	Radio
7	52	53.26		39	23	28.5		3	0.031	5.08	Radio
7	59	40.37		14	22	36.4		4	0.024	5.70	Radio
8	3	15.11		21	21	27.0		3	0.023	4.85	Radio
8	6	23.03		20	57	23.0		4	0.021	5.66	Radio
8	8	48.79		62	59	56.8		3	0.015	4.43	IR
8	8	49.40		66	51	53.0		4	0.029	4.75	none
8	16	49.41		52	53	31.5		4	0.029	5.23	none
8	20	36.58		2	18	13.4		4	0.026	5.16	none
8	23	9.43		26	53	4.3		4	0.026	5.93	Radio
8	23	15.64		29	15	36.2		3	0.015	5.25	Radio
8	24	22.27		26	47	11.0		4	0.028	5.78	Radio
8	37	24.85		13	12	58.1		4	0.020	6.68	none
8	41	50.45		19	7	1.9		4	0.028	6.35	none
8	42	1.67		19	16	0.0		4	0.018	5.15	none
8	47	20.79		51	35	20.6		3	0.037	4.94	none
8	48	44.58		33	26	47.4		4	0.085	5.65	Radio
8	52	28.67		6	17	4.2		4	0.039	5.15	Radio
8	59	0.82		-13	59	43.2		4	0.056	5.70	none
8	59	18.33		18	12	47.7		4	0.066	5.10	none
8	59	25.73		-13	47	9.8		3	0.067	5.48	IR
9	7	21.58		2	56	32.8		3	0.025	4.70	none
9	20	21.91		34	33	24.2		4	0.028	5.34	Radio
9	23	47.37		38	57	46.4		3	0.019	5.47	Radio
9	24	42.54		-5	31	40.1		3	0.019	5.22	Radio
9	26	27.61		-5	45	49.6		3	0.019	5.11	none
9	26	55.04		6	17	35.3		4	0.023	5.23	none
9	46	5.96		7	42	48.0		4	0.039	5.21	Radio
9	48	46.43		11	53	22.6		4	0.046	5.85	none
9	51	11.40		44	18	2.1		4	0.043	5.28	Radio
9	54	12.36		32	23	43.2		4	0.047	5.20	Radio
9	54	52.96		22	54	54.2		4	0.041	5.68	none
10	1	1.97		5	14	48.8		4	0.061	4.63	none
10	3	21.13		-29	45	42.3		4	0.049	5.10	Radio
10	4	14.22		1	7	27.6		3	0.035	4.66	none
10	9	47.67		35	16	57.3		4	0.050	5.08	Radio
10	15	36.57		1	18	50.8		4	0.039	5.27	none
10	20	56.40		-10	17	10.2		3	0.034	4.72	Radio
10	28	31.04		31	28	57.5		3	0.018	4.92	Radio
10	29	12.97		31	20	5.6		3	0.018	5.30	IR
10	30	28.42		9	18	34.9		4	0.036	5.95	Radio
10	40	42.63		56	14	45.3		3	0.034	4.92	none
10	43	4.99		9	22	40.3		4	0.022	5.28	none
10	45	52.61		6	59	18.9		4	0.048	5.76	Radio
10	47	12.77		7	0	47.5		3	0.046	5.41	Radio
10	49	22.60		-18	22	30.3		4	0.051	4.94	none
11	6	2.13		37	52	5.4		4	0.026	5.13	Radio
11	9	53.56		-26	17	41.9		4	0.021	5.83	none
11	9	58.96		35	55	37.3		3	0.023	5.11	Radio

TABLE 2. (continued)

R.A. (1950): ^h	^m	^s	Dec. (1950): [°]	[']	["]	Ap.	Flux	σ	ID
11	27	12.44	30	28	17.6	4	0.057	5.24	Radio
11	28	31.62	30	20	16.9	4	0.048	5.13	Radio
11	35	11.09	-8	48	28.6	4	0.033	5.09	none
11	37	51.74	28	59	59.9	3	0.015	4.45	Radio
11	39	2.69	34	25	35.6	3	0.026	4.65	Radio
11	39	24.37	66	11	36.6	3	0.016	4.43	none
11	43	45.37	-28	27	13.6	4	0.060	5.14	none
11	45	13.32	-10	12	55.8	3	0.045	4.75	none
11	45	50.07	0	59	42.0	3	0.017	4.63	Radio
11	56	8.83	-27	14	25.8	4	0.040	6.31	none
11	58	0.12	1	30	59.2	3	0.032	5.61	IR
11	58	40.38	-18	20	4.4	4	0.062	5.89	none
12	7	0.15	39	40	33.9	3	0.017	4.77	Radio
12	9	54.98	-1	15	42.3	3	0.019	4.50	IR
12	16	21.40	38	11	59.5	3	0.013	5.08	Radio
12	33	29.16	66	23	38.2	4	0.054	6.02	IR
12	38	39.03	-28	42	32.3	4	0.048	5.37	none
12	45	43.47	60	52	23.0	3	0.020	4.56	none
12	46	37.02	59	10	11.0	3	0.032	5.03	IR
12	48	37.52	0	-56	12.6	4	0.022	6.97	none
12	50	59.89	56	35	16.4	4	0.028	5.10	none
12	52	30.54	56	56	25.3	4	0.029	5.22	none
12	54	31.18	-5	28	18.4	3	0.008	4.56	none
12	57	13.92	30	53	17.6	4	0.040	4.52	Radio
12	58	32.65	35	51	39.0	3	0.009	6.59	Radio
12	59	6.63	31	12	48.4	4	0.054	4.73	Radio
13	0	4.87	-2	3	7.7	4	0.030	5.33	Radio
13	1	31.06	63	41	50.5	3	0.028	5.01	IR
13	3	42.55	-1	53	43.2	4	0.059	5.77	IR
13	12	12.22	29	10	31.4	4	0.023	5.10	Radio
13	14	26.05	28	58	3.5	4	0.031	5.68	Radio
13	14	56.39	-22	54	8.5	4	0.024	5.11	none
13	15	58.68	29	25	54.4	4	0.040	5.87	Radio
13	16	1.56	-22	40	14.2	3	0.026	4.86	none
13	18	19.67	70	36	17.2	4	0.038	5.24	Radio
13	22	44.32	-4	53	12.5	3	0.026	4.80	none
13	26	34.83	-8	26	59.5	4	0.084	5.17	none
13	27	30.44	59	1	8.2	3	0.019	4.52	Radio
13	32	8.82	41	22	41.5	3	0.020	4.96	Radio
13	35	58.45	52	16	52.8	4	0.044	5.13	Radio
13	37	44.48	67	50	38.0	3	0.025	4.77	Radio
13	45	55.13	40	9	23.1	4	0.033	4.76	Radio
13	52	11.12	40	18	37.2	4	0.042	5.13	Radio
13	52	48.09	0	50	51.9	4	0.051	5.62	Radio
14	0	29.57	62	11	49.5	4	0.059	5.00	none
14	1	15.92	64	33	40.9	4	0.031	4.89	IR
14	1	51.64	64	25	22.2	4	0.040	6.08	IR
14	4	28.96	72	33	24.2	4	0.051	6.62	IR
14	4	49.80	22	30	18.5	4	0.047	4.97	none
14	9	44.02	52	8	55.8	4	0.025	6.85	none
14	13	19.45	19	19	55.1	3	0.035	4.51	Radio
14	18	26.16	72	20	37.5	4	0.044	5.12	Radio
14	21	11.06	-18	21	27.0	4	0.033	5.46	none
14	22	13.70	1	38	4.3	4	0.061	6.05	none
14	22	18.85	52	13	9.3	3	0.015	4.34	IR
14	25	47.29	1	48	6.6	4	0.026	5.40	none
14	28	23.15	62	12	57.0	3	0.030	4.83	none
14	28	32.21	62	31	3.8	4	0.033	5.17	Radio
14	32	26.51	-17	31	23.1	4	0.058	5.46	none
14	32	53.75	-18	51	20.1	3	0.052	4.77	none
14	33	35.50	19	37	4.2	4	0.054	5.94	none
14	42	1.86	27	5	7.8	4	0.031	5.85	none
14	42	53.91	52	7	33.0	3	0.018	4.83	IR
14	43	48.75	12	3	7.1	3	0.019	4.64	none
14	50	43.11	21	16	12.6	4	0.023	5.73	Radio
14	52	20.84	16	3	19.6	4	0.078	5.58	none
14	53	16.00	21	23	44.1	4	0.032	6.45	Radio

TABLE 2. (continued)

R.A. (1950):	<i>h</i>	<i>m</i>	<i>s</i>	Dec. (1950):	<i>°</i>	<i>'</i>	<i>"</i>	Ap.	Flux	σ	ID
14	57	7.18		4	29	46.7		4	0.045	5.28	Radio
14	58	52.12		71	35	58.7		4	0.039	5.91	Radio
14	59	55.27		2	39	14.1		4	0.063	5.82	none
15	1	47.88		-32	55	25.1		4	0.040	5.20	none
15	2	10.38		26	27	32.5		4	0.022	5.21	none
15	2	43.57		22	10	13.3		3	0.018	4.51	none
15	4	40.10		11	2	52.3		4	0.029	6.11	Radio
15	8	43.10		57	28	7.1		4	0.057	5.54	Radio
15	12	55.21		33	27	32.3		4	0.023	5.07	none
15	15	28.58		22	55	20.4		4	0.042	5.28	Radio
15	17	11.63		20	17	3.6		4	0.014	5.42	none
15	20	31.67		71	43	23.8		4	0.060	5.10	Radio
15	23	7.30		30	1	50.4		3	0.027	5.41	Radio
15	24	47.65		22	57	55.0		4	0.025	5.33	none
15	25	26.51		11	19	23.3		4	0.038	5.18	none
15	25	41.61		10	22	39.6		4	0.046	5.35	none ^b
15	28	22.56		10	51	59.5		4	0.049	5.11	none
15	28	34.36		69	51	48.0		4	0.022	5.33	IR
15	29	48.69		-8	31	14.3		3	0.023	4.70	none
15	31	1.85		1	34	31.9		4	0.025	4.83	none
15	31	39.46		31	37	41.3		3	0.012	4.69	Radio
15	31	46.93		1	55	27.1		3	0.029	4.53	none
15	32	16.15		13	42	51.2		4	0.065	5.26	none
15	32	20.00		31	40	7.1		3	0.027	5.96	Radio
15	32	31.36		13	23	49.6		4	0.067	5.09	none
15	33	51.79		23	28	27.1		3	0.015	6.40	none
15	39	4.35		66	8	33.3		2	0.013	4.39	Radio
15	44	36.56		-17	2	39.4		4	0.061	5.15	none
15	47	19.04		5	52	30.5		4	0.074	6.27	Radio
15	48	15.32		5	21	18.0		4	0.062	5.41	Radio
15	50	19.31		-4	43	41.4		4	0.029	5.13	none
15	59	33.46		41	13	3.8		4	0.014	5.25	Radio
16	3	12.51		66	54	59.9		3	0.020	5.50	none
16	5	32.26		30	8	25.3		4	0.048	5.31	Radio
16	6	8.28		17	24	50.9		4	0.030	6.07	IR
16	6	22.79		17	24	31.6		3	0.015	4.66	IR
16	7	3.15		10	48	46.4		4	0.097	5.73	none
16	7	31.38		66	11	51.1		4	0.029	5.36	none
16	7	48.37		-18	25	27.1		3	0.014	5.21	none
16	14	4.12		6	21	59.0		3	0.064	4.84	IR
16	15	14.68		32	17	20.7		4	0.025	5.12	Radio
16	18	20.56		5	42	51.9		3	0.042	4.55	none
16	22	25.42		23	37	51.8		3	0.018	4.50	IR
16	23	1.40		26	40	33.1		3	0.006	4.84	IR
16	23	34.47		61	21	55.5		3	0.037	5.17	none
16	25	33.18		41	11	0.4		4	0.036	4.62	Radio
16	26	20.36		15	16	24.7		3	0.033	4.68	none
16	31	24.18		5	39	44.9		4	0.062	5.22	none
16	35	47.60		12	9	43.2		3	0.016	5.06	none
16	36	6.70		11	45	13.0		4	0.033	5.10	Radio
16	43	18.10		-3	21	48.1		4	0.025	5.47	none
16	44	38.65		32	33	7.0		4	0.021	5.04	Radio
16	46	46.78		71	5	4.8		4	0.065	5.26	Radio
16	48	33.10		5	21	26.6		3	0.007	4.73	Radio
16	54	40.05		9	44	6.7		4	0.036	6.01	Radio
16	54	41.27		9	18	34.8		4	0.025	5.13	IR
16	55	43.98		35	9	23.8		3	0.014	5.95	Radio
17	2	2.92		33	59	29.5		3	0.025	6.29	IR
17	3	38.88		0	43	36.6		3	0.025	4.53	none
17	3	43.35		23	46	56.4		3	0.019	4.50	none
17	6	44.97		49	8	19.9		4	0.059	6.41	none
17	7	10.54		54	47	34.9		4	0.053	5.55	none
17	8	0.37		39	41	57.5		4	0.058	6.07	Radio
17	11	18.87		48	41	57.6		3	0.031	4.96	Radio
17	17	57.25		32	37	32.1		4	0.038	5.85	Radio
17	18	55.76		32	49	43.1		4	0.029	5.06	Radio
17	20	44.53		34	15	34.1		3	0.035	4.33	Radio

TABLE 2. (continued)

R.A. (1950): ^h	<i>m</i>	<i>s</i>	Dec. (1950): ^o	<i>'</i>	<i>"</i>	Ap.	Flux	σ	ID
17	22	25.09	66	57	32.2	4	0.066	4.67	Radio
17	28	28.45	52	33	1.0	4	0.066	5.28	Radio
17	29	36.53	52	34	51.6	3	0.050	4.51	Radio
17	39	57.78	52	29	36.7	4	0.053	5.16	Radio
17	45	11.74	27	33	51.4	4	0.019	5.34	none
17	45	57.58	69	20	29.1	4	0.071	5.36	Radio
17	49	58.60	70	46	1.0	4	0.147	5.82	Radio
17	56	51.43	63	53	10.2	4	0.089	6.00	Radio
17	58	26.93	64	9	33.9	4	0.052	5.12	Radio
18	9	57.25	78	22	45.1	3	0.028	4.59	none
18	10	44.47	64	31	54.5	4	0.190	5.17	IR
18	20	47.03	64	1	23.5	4	0.072	5.42	Radio
18	28	8.09	64	2	18.0	3	0.058	5.51	Radio
18	32	35.04	64	47	32.4	4	0.161	6.40	Radio ^c
19	13	38.60	67	54	56.8	4	0.032	6.14	none
19	52	14.64	-69	12	30.0	3	0.018	4.52	Radio
19	54	1.24	-69	25	26.5	3	0.024	4.81	none
20	6	42.77	-36	8	23.2	4	0.048	5.24	none
20	11	8.07	-60	8	40.8	4	0.057	5.10	none
20	15	3.37	-3	37	41.2	4	0.042	5.03	none
20	55	5.42	-5	7	33.9	4	0.031	5.57	none
21	13	58.27	5	14	11.9	3	0.024	5.12	IR
21	18	12.17	-11	14	50.2	4	0.018	5.06	none
21	20	27.80	16	33	37.6	4	0.029	6.64	Radio
21	22	11.46	5	19	51.6	3	0.037	4.69	none
21	22	42.46	10	5	23.9	3	0.027	5.06	Radio
21	27	24.85	4	35	37.0	4	0.062	5.47	none
21	42	47.71	9	30	8.1	4	0.044	5.33	none
21	42	58.05	3	42	20.6	3	0.009	4.59	none
21	42	59.85	22	25	58.1	3	0.030	5.35	none
21	48	15.66	14	47	12.6	4	0.030	5.10	none
21	52	48.78	-61	2	44.1	4	0.069	5.11	IR
21	55	59.96	3	42	3.1	4	0.025	7.37	none
22	1	4.33	16	56	59.0	4	0.027	5.18	none
22	1	49.32	17	5	16.7	4	0.031	5.60	none
22	6	50.74	-4	24	46.0	3	0.019	4.85	none
22	35	11.48	-15	41	36.7	4	0.050	5.63	none
22	48	58.93	31	22	3.6	2	0.012	4.13	none
22	52	23.37	15	48	38.6	4	0.034	4.55	IR
22	55	27.03	20	18	47.8	3	0.020	4.87	none
23	3	28.01	14	50	39.6	4	0.043	5.42	none
23	3	37.52	-23	30	44.1	4	0.039	6.56	none
23	4	30.93	24	56	11.7	4	0.035	5.56	none
23	9	43.75	-49	51	4.3	3	0.017	4.35	none
23	10	52.80	-50	11	15.0	4	0.025	5.01	none
23	11	51.53	-50	3	51.6	4	0.030	5.21	none
23	12	32.66	-42	39	13.9	4	0.059	5.43	none
23	15	30.72	15	31	47.7	4	0.049	5.52	Radio
23	17	38.78	-42	40	36.0	4	0.051	5.31	none
23	48	14.24	19	36	52.4	4	0.040	6.44	none
23	50	36.90	28	46	42.4	4	0.046	5.14	none
23	57	38.75	29	49	46.1	4	0.041	5.88	IR
23	58	23.84	29	27	14.5	4	0.035	4.75	Radio

^aThis source is coincident with RASS Bright Source J010954.5-151018.

^bThis source is coincident with RASS Bright Source J152807.3-101035.

^cThis source is coincident with RASS Bright Source J183231.5+644949.

Notes to TABLE 2

The Ap. column indicates the best aperture used to approximate the source extent. A value of 2 corresponds to 2.35', 3 to 4.2', and 4 to 6.1'. Flux is in units of counts per second, and the ID column indicates whether NED found a radio source, an infrared source or neither within 12' of the EXSS source.

ter catalog of 7419 sources prior to the selection of extended sources, 152 sources coincide with EMSS stars, 313 with AGN and 28 with BL Lac objects. In addition, 79 sources in the master catalog coincide with EMSS galaxy clusters. In

contrast, the EXSS (the catalog filtered for extended sources) has only 6 sources coincident with EMSS stars, 15 with AGN and 1 with a BL Lac object. That is, only about 4% of the 493 objects known to be point-like make it through the

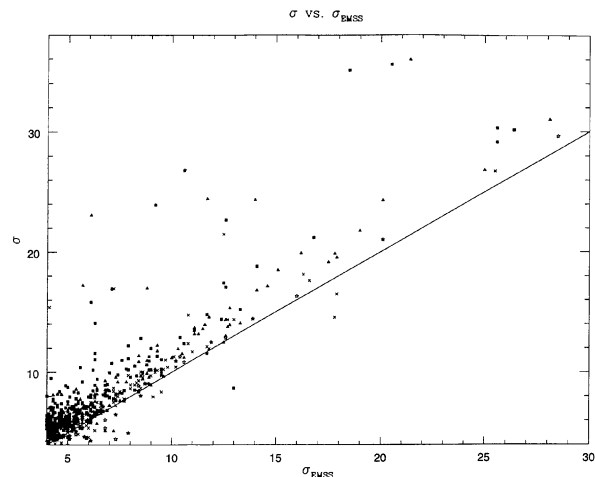


FIG. 5. Plot of σ vs σ_{EMSS} for all sources in the master catalog with corresponding EMSS detections. A subset of these sources are also in the EXSS catalog and are shown in the next figure. Solid squares represent aperture 4 sources. Solid triangles represent aperture 3 sources, while crosses and open stars represent aperture 2 and aperture 1 sources respectively. The diagonal line indicates where σ equals σ_{EMSS} . See Sec. 4 for further discussion.

“cutoff ratio” filters. In contrast, we retained 27% of the clusters after the application of the filters.

Finally, a cross correlation of the EXSS catalog with the recently published *ROSAT* All Sky Survey Bright Source Catalog (hereafter called BSC; Voges *et al.* 1996) yields interesting results. Of the 146 matches, 68% have the extended source flag set in the BSC catalog. Figure 7 shows that the EXSS aperture number is roughly consistent with the BSC source extent parameter. Among the unidentified portion of the EXSS catalog, only 3 sources are coincident with BSC sources. These are noted in Table 2.

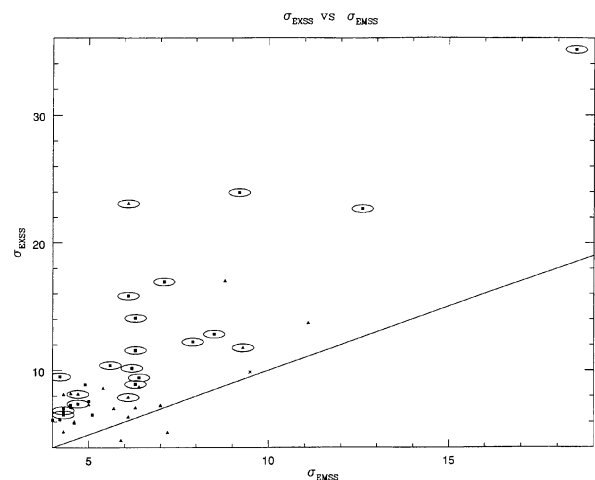


FIG. 6. Plot of σ_{EXSS} vs σ_{EMSS} . Symbols have the same meaning as in Fig. 5. This plot only shows extended sources (sources in the EXSS). See Sec. 4 for further discussion.

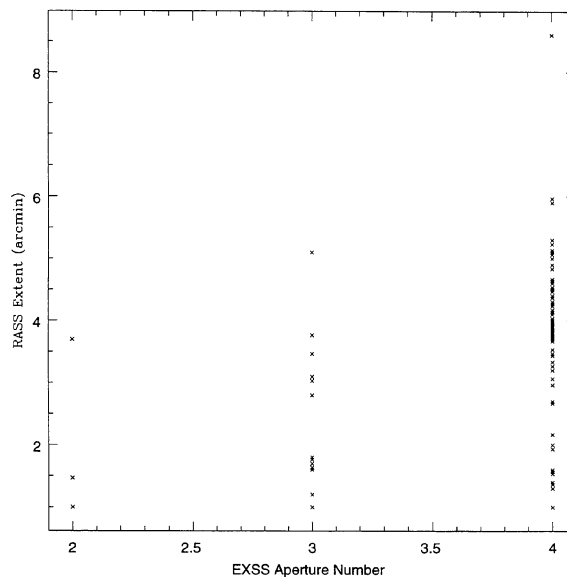


FIG. 7. EXSS aperture number vs RASS source size. Aperture number 2 corresponds to 2.35', aperture 3 to 4.2', and aperture 4 to 6.1'.

5. CONCLUSIONS

Using careful flat-fielding and source extraction techniques, we have derived from the *Einstein* IPC database a catalog of candidate extended X-ray sources. Several hundred of these are identified with previously cataloged clusters of galaxies, nearby galaxies, and other extended sources of X-ray emission. There remain 321 candidates, however, without optical identifications. Nearly all of those bright enough to be detected in the BSC are seen, and over two-thirds are listed as extended in that survey. Thus, this catalog provides a rich source of targets for optical followup programs designed to construct complete samples of X-ray-selected clusters of galaxies. Observations of this sample can be expected to be of value in assessing the incompleteness of optical cluster catalogs and, to the extent that they represent a more distant sample, in charting the X-ray evolution of galaxy clusters.

For those who wish to use the catalogs (either the large main catalog, the EXSS catalog, the unidentified part of the EXSS catalog or the catalog of sources appearing in only one aperture) in electronic form, they are available on the internet at <http://astro.caltech.edu/~bro>.

This research has made use of the High Energy Astrophysics Science Archive Research Center, provided by the NASA-Goddard Space Flight Center and the NASA/IPAC Extragalactic Database (NED) which is operated by the Jet Propulsion Laboratory, Caltech, under contract with the National Aeronautics and Space Administration. B.R.O. is supported by a National Science Foundation Graduate Research Fellowship and Futdi. This work was supported at Columbia by the National Aeronautics and Space Administration under contract NAS5-32063, and is Contribution Number 626 of the Columbia Astrophysics Laboratory.

REFERENCES

- Beichman, C.A., Neugebauer, G., Habring, H. J., Clegg, P. E., & Chester, T. J. (eds.) 1988, *IRAS Catalogs and Atlases* (National Aeronautics and Space Administration, Washington, D. C.)
- Elvis, M. 1990, *Imaging X-ray Astronomy* (Cambridge University Press, Cambridge)
- Giacconi, R., *et al.* 1979, *ApJ*, 230, 540
- Gioia, I. M., & Luppino, G. A. 1994, *ApJS*, 94, 583
- Gioia, I. M., Maccacaro, T., Schild, R. E., Wolter, A., Stocke, J. T., Morris, S. L., & Henry, J. P. 1990, *ApJS*, 72, 567
- Gregory, P. C., & Condon, J. J. 1990, *The 87GB Catalog of Radio Sources* (National Radio Astronomy Observatory, Greenbank, WV)
- Hamilton, T. T., Helfand, D. J., & Wu, X. 1991, *ApJ*, 379, 576
- Henry, J. P., Gioia, I. M., Maccacaro, T., Morris, S. L., Stocke, J. T., & Wolter, A., 1992, *ApJ*, 386, 408
- Moran, E. C., Helfand, D. J., Becker, R. H., & White, R. L. 1996, *ApJ*, 461, 127
- Pesce, J. E., Fabian, A. C., Edge, A. C., & Johnstone, R. M. 1990, *MNRAS*, 244, 58
- Röser, S. & Bastian, U. 1991, *The PPM Star Catalogue* (Spektrum Akademische Verlag, Heidelberg)
- Stocke, J. T., Morris, S. L., Gioia, I. M., Maccacaro, T., Schild, R., Wolter, A., Fleming, T. A., & Henry, J. P. 1991, *ApJS*, 76, 813
- Tucker, W. H., Tananbaum, H., & Remillard, R. A. 1995, *ApJ*, 444, 532
- Voges, W., *et al.* 1996, *A&A* (in press)